JOURNAL OF HIGH-FREQUENCY COMMUNICATION TECHNOLOGIES
Vol. 01 (01) (2023), pp.01-11

A Tri-band Dual Substrate Aperture Coupled Microstrip Antenna for C, X, and Ku Band Applications

Jasmine Vijithra Ayyappan[1*], Milton Arulappan[2], Beno Austin Dharma Raj[3]

[1] Department of ECE, Sri Sivasubramaniya Nadar College of Engineering, Kalavakkam, Chennai, 603110, India, *E-mail address: jasminevijithraa@ssn.edu.in, jasece46@gmail.com*
[2] Department of ECE, St. Xavier's Catholic College of Engineering, Nagercoil, Tamil Nadu, India, *E-mail address: milton@sxcce.edu.in*
[3] Department of ECE, Dr. Sivanthi Aditanar College of Engineering, Tiruchendur, Tamil Nadu, India, *E-mail address: beno@drsacoe.com*

Abstract

The design work presents a triple Y-fed dual substrate aperture coupled microstrip antenna that operates in C, X, and Ku bands. The overall dimension of the antenna is 50 mm x 40 mm x 1.894 mm. The antenna has four layers with two dissimilar substrates. A unique triple Y-structured feed line connected to a quarter-wave transformer forms the first layer of the design and shows a greater impact on impedance matching. A superimposed modified defective ground structure is sandwiched between two dissimilar substrates, FR4 and RT5880. The FR4 substrate is placed above the triple-Y feed structure, over which a superimposed defected ground structure (DGS) is placed to obtain enhanced bandwidth. The third layer is formed by placing the second substrate, RT5880, above the ground plane. The dielectric constant of the lower substrate is considered higher than the upper substrate to avoid undesired radiation at unwanted frequencies. A patch with three rectangular slots is placed over the RT5880 substrate for its tri-band characteristics. The patch is excited effectively through the slots in the ground plane, thereby enhancing the coupling between the patch and the feed and resulting in maximum radiation of radio frequency energy. With this, an enhanced bandwidth of 12.66 %, 16.67 %, and 7.19 % in all three bands is attained. Besides, the proposed design has a gain of 3.265 dBi at the C band, 3.305 dBi at the X band, and 4.385 dBi at the Ku band. The fabricated antenna is tested, and the results are compared for both simulated and measured values. The results emphasize that a tri-band antenna can be used effectively at various operating frequencies, including the fifth-generation wireless application band.

Keywords: *Aperture coupled, bandwidth, defected ground structure, quarter wave transformer*

1. Introduction

Microstrip antennas have received high attention due to their low structural complexity, lightweight, compatibility, low cost, and easy fabrication. This antenna incorporates various feed techniques

[*]**Corresponding author**
Received: 15^{th}, December 2022, Revised: 03^{rd} January, 2023 Accepted: 08^{th} January 2023 and available online 26^{th} January 2023
https://doi.org/10.58399/GTMX8376

This work is licensed under a Creative Commons Attribution 4.0 License(CC BY 4.0).
For more information, see https://creativecommons.org/licenses/by/4.0/

like line feed, probe feed, aperture coupled feed, and proximity coupled feed. Aperture-coupled feeding techniques, in particular, have an advantage over other techniques as they are less sensitive to spurious radiations As a result, massive improvements can be seen in gain attainment, bandwidth enhancement, coupling efficiency, and return loss improvement. However, microstrip patch antennas have the serious disadvantage of having a narrow bandwidth and low-frequency sensitivity. Due to this bandwidth enhancement and efficiency improvement, using microstrip antennas becomes the biggest challenge. To overcome this, a simple solution is provided in this paper that improves bandwidth and gain with good coupling efficiency.

In (Khan et al., 2018), the empty substrate integrated waveguide (ESIW) technique is used as a feed element. Though it enhances efficiency, the attainment of bandwidth is about 6.8% (at 27.4–29.3 GHz) and 5% (at 27.3–28.7 GHz). In (Li et al., 2017) a multibeam array technique using an aperture-coupled antenna is proposed. This work uses a multilayer feed with vertical SIW interconnections as a feeding network resulting in structural complexity leading to a very minimal amount of radiation of beams. Other techniques include liquid crystal-based aperture-coupled antennas (Kim and Oh, 2020) and cavity-back slotted coupled antennas with dual slant polarization (Yang et al., 2021) are reported in developing an aperture-coupled radiator.

However, less efficiency is noted in the work reported by (Kim and Oh, 2020) and (Yang et al., 2021). Though (Kim and Oh, 2020) gives a wide bandwidth of 16% (at 27–29 GHz), the gain attainment is low. Similarly, (Yang et al., 2021) shows a narrow bandwidth of 6% (at 27.2–28.9 GHz). In (Liu et al., 2019), a low-profile antenna is discussed for TM12 and TM30 modes. Though the radiation characteristics are improved, the design thickness is not compatible. Bandwidth enhancement in the aperture-coupled antenna is brought by a metamaterial-based slotted grid (Liu et al., 2015), (Bancroft, 2019), (Balanis, 2009) and gain enhancement using the coupling aperture (Zhang et al., 2017). A few other techniques like a cavity-backed slotted coupled antenna (Rao and Johnston, 2004), inverted feeding structures with three substrate layers (Yun and Yoon, 2005), wideband 180° coupler as feed (Honari et al., 2018), shared aperture for dual-band (Liu et al., 2019)-(Wang and Huang, 2020), and a folded loop with a meandering inverted F antenna (Hong et al., 2014) are reported to improve the radiation performance of the aperture-coupled antenna. However, narrow bandwidth of 3% (at 3.8–3.9 GHz) (Rao and Johnston, 2004), complex structures (Yun and Yoon, 2005), (Honari et al., 2018), (Ding and Cheng, 2020), less efficiency (Liu et al., 2019), (Wang and Huang, 2020), (Ding and Cheng, 2020), and low return loss, less gain, and efficiency (Hong et al., 2014) are observed.

In this paper, we propose the design of a low-profile tri-band aperture coupled microstrip antenna with two dissimilar substrates. Specifically, the proposed design covers the C, X, and Ku bands of frequency. A triple Y-structured feed and a modified defected ground structure are the key factors in obtaining perfect impedance matching by avoiding spurious feed radiations.

The proposed design can be used for various applications related to fifth-generation (5G) frequencies, like microwave landing systems (5.00–5.2 GHz), unarmed aircraft (5.03–5.09 GHz), space research services (5.25–5.57 GHz), direct broadcast satellite services (10–14 GHz), Wi-Fi (802.11a) (5.15–5.35 GHz), mobile WiMAX (802.16e) (4.8–5.47 GHz), RLAN earth services (5.2–5.3 GHz), space-to-earth satellite services (11.7–12.2 GHz), earth-to-space satellite services (14.0–14.5 GHz), and 5G mobile communication purposes. Section 2 describes the design of a single-element aperture coupled antenna that operates at tri-band frequencies.

The structural modification of the antenna elements and its bandwidth accomplishment concerning each modification are discussed. The final design is fabricated and tested. The antenna performance is compared with the literature, and the advancement in results is highlighted.

2. Design of Tri-band aperture coupled Dissimilar Dual Substrate Microstrip Antenna

The main focus of the design is to achieve bandwidth enhancement in the C, X, and Ku bands of frequency through the aperture coupling technique. On analyzing the other feeding techniques of microstrip antennas, the accuracy of obtaining higher bandwidth is remarkable in the aperture-coupled technique. The design competency has been explained in the following sections.

2.1. Design of Dual Substrate Aperture-Coupled Antenna Rectangular Slots, Defected Ground Structure, and Triple Y-feed

The schematic of the proposed design is shown in Fig.1. The aperture-coupled antenna is designed for a cut-off frequency of 5 GHz. The proposed design has two dissimilar substrates that are sandwiched between the feed line, ground plane, and patch. The substrate below the patch is RT5880 of thickness 0.254 mm, and the dielectric constant is 2.2. The substrate below the ground plane is FR4 of thickness 1.57 mm, and the dielectric constant is 4.4. Here, the dielectric constant of the lower substrate is considered greater than the dielectric constant of the upper substrate (i.e., value of FR4 $>$ value of RT5880) to achieve a narrow bandwidth and eliminate spurious radiations at undesired frequencies.

Between the two substrates is the ground plane with a modified superimposed defected structure, which is shown in Fig. 2. On the ground plane, horizontal and vertical slots are made and connected. For proper matching, the length of the slots and the spacing between each horizontal slot in the ground plane are both half-wavelength. The dimension of the horizontal slots is 18 mm x 0.75 mm and the size of the vertical slots is 2.6 mm x 20.11 mm. The spacing between each slot is so carefully designed such that the mutual coupling between the slots remains undisturbed to avoid reflections and sidelobes. A narrow rectangular slit of size 1.5 mm x 1 mm, followed by a square slot of size 1.5 mm x 1.5 mm, is brought into the ground plane.

A line feed cannot excite the slots in the ground plane, resulting in mismatching and poor performance. To overcome this, various feed structures like series feed, corporate feed, and line feed are analyzed. A triple-Y feed structure has been implemented due to its exceptional matching properties. In Fig. 3, a quarter wave transformer is used in the main feed arm to obtain a larger bandwidth. The angle between the arm and stem of the feed is 45°, and the angle between the broadside arms is 90°. All the arms of the Y feed are the same length (e) 8.2 mm and width (d) 1.5 mm. The arms provide a high inductive effect such that more energy is transferred to the patch, allowing it to radiate effectively.

Figure 4 depicts the layout of the patch with three rectangular slots. Initially, the patch is designed for an operating frequency of 5 GHz. By increasing the width of the patch, the edge conductance can be increased, so that 50 Ω impedance matching can be obtained.

To improve the antenna's bandwidth and radiation characteristics, three rectangular slots are etched into the patch that covers the new operating frequencies of 11.5 GHz and 14.2 GHz. These slots introduce a capacitive effect in the rectangular patch, which is responsible for the maximum current distribution throughout the patch. Since the feed line incorporates an inductive effect, the edges of the patch radiate effectively, resulting in the wide performance of the antenna. Figure 5 illustrates the variation in the s parameter concerning the changes in the patch and defected ground structure (DGS).

The patch without slots resonates at 9 GHz and 11.5 GHz. To make the patch resonate at a 5 GHz frequency, the horizontal slot at the center of the ground plane is replaced with defective ground structures comprising horizontal and vertical slots. Later, a rectangular slot is introduced in the patch such that the design satisfies the cut-off frequency criteria.

To resonate at 11.5 GHz and 14.2 GHz, two rectangular half-wavelength slots are introduced at the patch. The DGS is modified such that spurious radiation is avoided and exact results are obtained.

3. Design Methodology

The width and length of the patch and substrate are designed using the conventional formulas for antenna design (Li et al., 2017). To increase the gain of the antenna, the resonant length is computed using Eq. 1 (Li et al., 2017)

$$L = \frac{c}{2f_r\sqrt{\epsilon_e}} - 2\Delta l \tag{1}$$

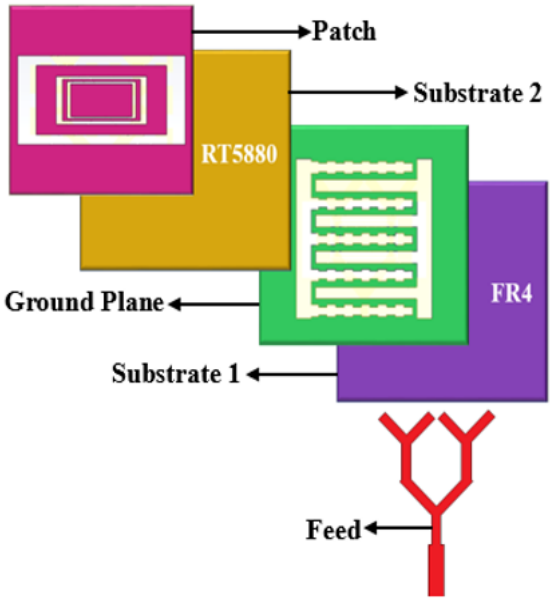

Figure 1. Schematic of Aperture Coupled Antenna with Modified Defected Ground Structure and a Patch with Three Rectangular Slots

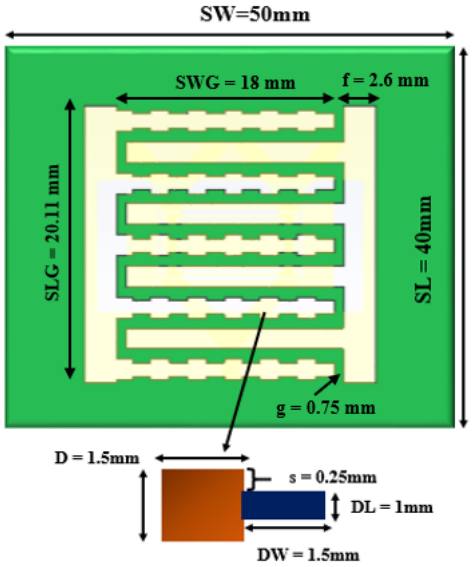

Figure 2. Modified Defected Ground Structure

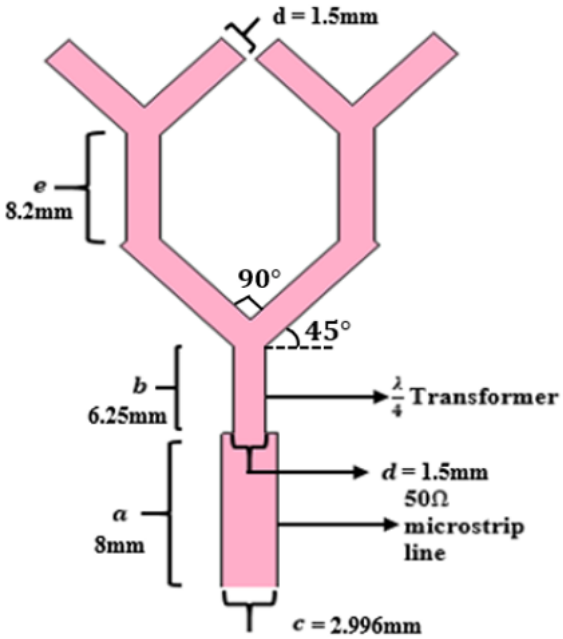

Figure 3. Structure of Y Feed with Quarter Wave Transformer

where f_r is the resonant frequency in gigahertz, ϵ_e is the effective dielectric constant, and Δl is the incremental length of the patch in millimeters. Here, the value of the effective dielectric constant is 2, which is less than the dielectric constant of RT5880 (2.2). The length and width of the rectangular slots are calculated using Eqs. 2 and 3 (Li et al., 2017), respectively:

$$L_x = 3\lambda \tag{2}$$

$$L_y = 2\lambda \tag{3}$$

where,

$$\lambda = \frac{c}{f_r \sqrt{\epsilon_e}}$$

Initially, the rectangular slots in the patch are created and fed from a single horizontal slot in the ground plane with a length of $\lambda/2$. With a normal line feed, it is found that the radio frequency (RF) source is not perfectly coupled to the patch due to poor matching. Also, the feed and the slot in the ground plane become insufficient to excite the slots in the patch.

Thus, there is a need for effective feeding techniques with perfect ground structure. The triple Y feed structure and superimposed defected ground structure concepts result from this. On integrating the DGS into the patch, the RF signals get transmitted to the defected structure, resulting in effective coupling between the DGS and the top surface of the patch. In addition, DGS also impacts the direction of current flow in the ground plane, which directly influences the S parameter values of the patch. To obtain perfect coupling, periodic square slots are made and connected through the periodic rectangular slots in the left half of the DGS, which in turn offers a change in the effective capacitance and inductance of the ground plane.

The dimensions of the periodic slots in the ground plane are finalized by the trial-and-error method with their corresponding wavelengths. The effect of a triple Y-fed modified DGS and patch with three rectangular slots is studied with the help of the surface current distribution shown in Fig. 6. At the surface of the patch and in between the slots in the ground plane, the current is evenly distributed.

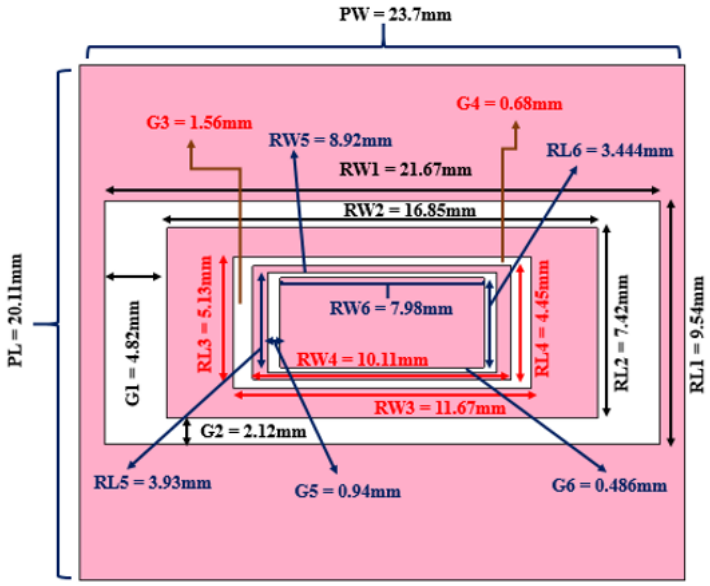

Figure 4. Structure of Patch with Three Rectangular Slots

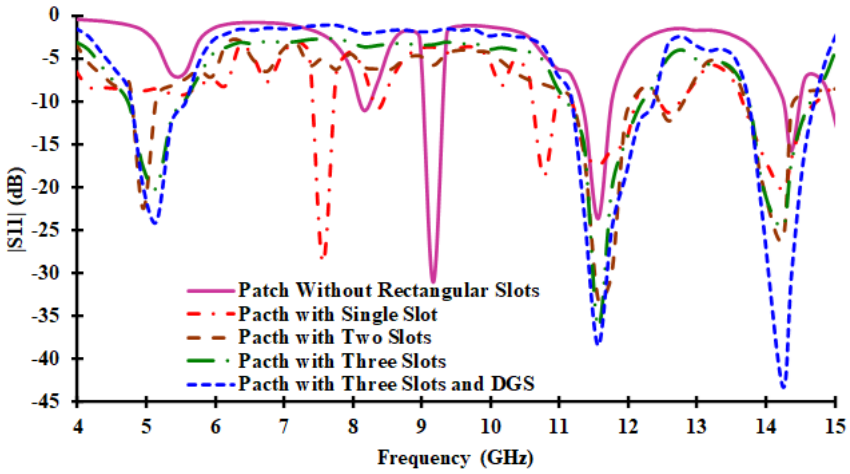

Figure 5. S Parameter Analysis for Various Configurations of Patch and DGS

The slots in the patch radiate more RF energy due to the perfectly matched DGS. The triple Y feed covers the overall surface area of the patch and DGS, thus satisfying the power requirements of the patch.

4. Results and Discussions

The proposed design is fabricated based on the optimized measurements and tested in the anechoic chamber. The fabricated prototype is shown in Figs. 7 (a)–(c), and the testing of the proposed design is shown in Fig. 7 (d). The three rectangular slots are etched on the patch and placed over the substrate RT5880. The modified DGS is so carefully designed to avoid more loss in the etching process of the proposed antenna. The simulated results are compared with the measured results to justify the performance of the proposed antenna in terms of bandwidth and gain attainment. Figure 8 (a) illustrates a comparative analysis between the measured and simulated results of S parameters, gain, and efficiency.

The simulated result shows a maximum resonant peak of 43.25 dB, whereas the measured

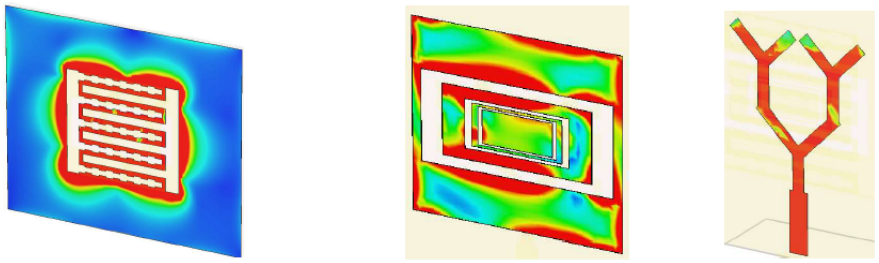

(a) (b) (c)

Figure 6. Surface Current Distribution at 5 GHz. (a) Defected Ground Plane, (b) Patch with Three Rectangular Slots, and (c) Triple Y Feed

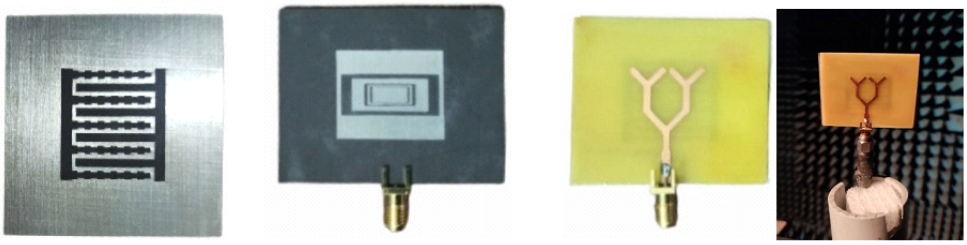

(a) (b) (c) (d)

Figure 7. (a) Defected Ground Structure of the Proposed Antenna, (b) Patch with Three Rectangular Slots, (c) Proposed Triple-Y Feed Structure, and (d) Testing of Proposed Antenna in Anechoic Chamber

result shows a maximum resonant peak of 40.6 dB. The bandwidth is also analyzed from the S curve of the proposed antenna, and it is observed that the measured bandwidth compromises with the simulated bandwidth with a negligible difference. From Fig. 8 (b), it is observed that a peak gain of $>$ 4 dBi is achieved with an average total efficiency of $>$ 82% for both measured and simulated values. Figure 9 showcases the performance of the proposed antenna in terms of radiation characteristics. The analysis is done using polar plots at three resonant frequencies.

Table 1. Comparison of Radiation Characteristics of Complete Design Process of Aperture Coupled Antenna with Final Output

Parameters	**Simulated Values**			**Measured Values**		
Freq (GHz)	5	11.5	14.2	5	11.5	14.2
BW (%)	13.6	9.5	7.9	12.6	9.7	7.2
Realized Gain (dBi)	3.5	4.12	4.6	3.11	3.75	4.25
$S_{11}(dB)$	-20.9	-36.2	-40.9	-21.9	-35.9	-41

The E and H plane patterns for the proposed antenna are analyzed separately for all three resonant frequencies and are compared with the measured results. The radiation patterns obtained are similar to the broadside pattern and the dipole eight pattern. The plot symbolizes the coherence between both values, which satisfies the output performance of the proposed antenna.

In Table 1, the measured and simulated radiation characteristics of the patch are compared. At center frequencies of 5 GHz, 11.5 GHz, and 14.1 GHz, the simulated gain values are 3.5 dBi, 4.12 dBi, and 4.6 dBi, respectively. However, the measured values are 3.11 dBi, 3.75 dBi, and 4.25 dBi. The simulated percentage bandwidth attained is 13.6% (4.8–5.5 GHz), 9.5% (11–12.1 GHz), and 7.9% (13.4–14.5 GHz), whereas the measured bandwidths are 12.6% (4.85–5.5 GHz), 9.7% (10.7–11.8 GHz), and 7.2% (13.3–14.3 GHz).

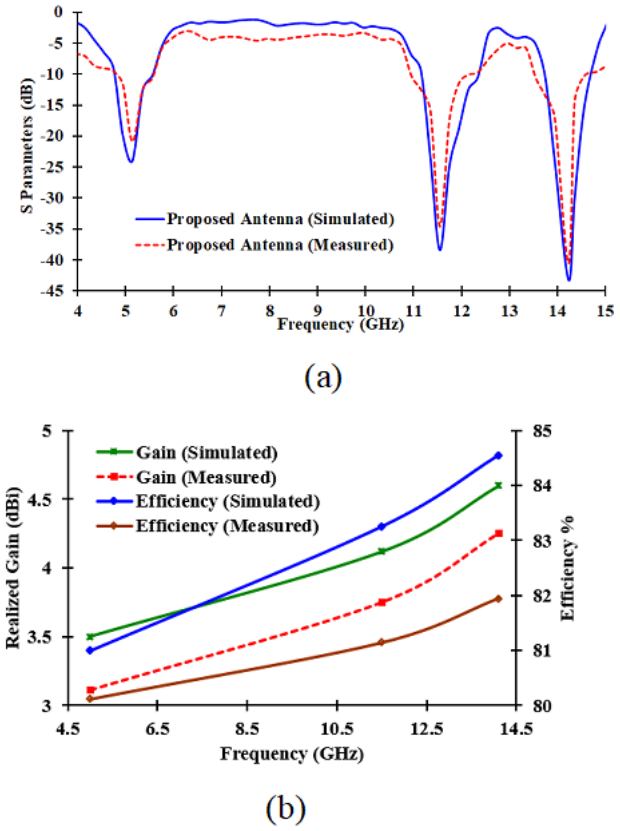

Figure 8. (a) Comparison of Measured and Simulated S Parameters of Proposed Antenna and (b) Gain and Efficiency Comparison of both Simulated and Measured Results

A minor deviation between the measured and simulated values is noted, which is due to the fabrication losses of the antenna. Besides, the proposed design is compared with the existing literature in Table 2 to highlight its advantages. The proposed design shows equally improved bandwidth in all three bands with reasonable gain. Besides, it shows efficiency >80%, which is comparatively higher than the cited works.

Table 2. Comparison of Proposed Design with Literature

References	**Sizes**	**Frequencies (GHz)**	**% BW**	**% Eff**	**Gain (dBi)**	**Elements**
(Khan et al., 2018)	$0.25\lambda \times 0.39\lambda$	28	3.5	> 88	6.57	Array
(Li et al., 2017)	$\lambda \times \lambda$	60	16.4	$35 - 40$	10	Array
(Rao and Johnston, 2004)	$3.6\lambda \times 2.9\lambda$	1.562 3.948	1.3 6.5	NA	NG	Single
(Liu et al., 2019)	$0.55\lambda \times 0.55\lambda$	16.5 33.25	10.7 9.1	> 64 > 55	3 4.5	Single
(Ding and Cheng, 2020)	$4.2\lambda \times 1.8\lambda$	2.4 5.2	21 5.7	> 74 > 76	12.29 12.29	Array

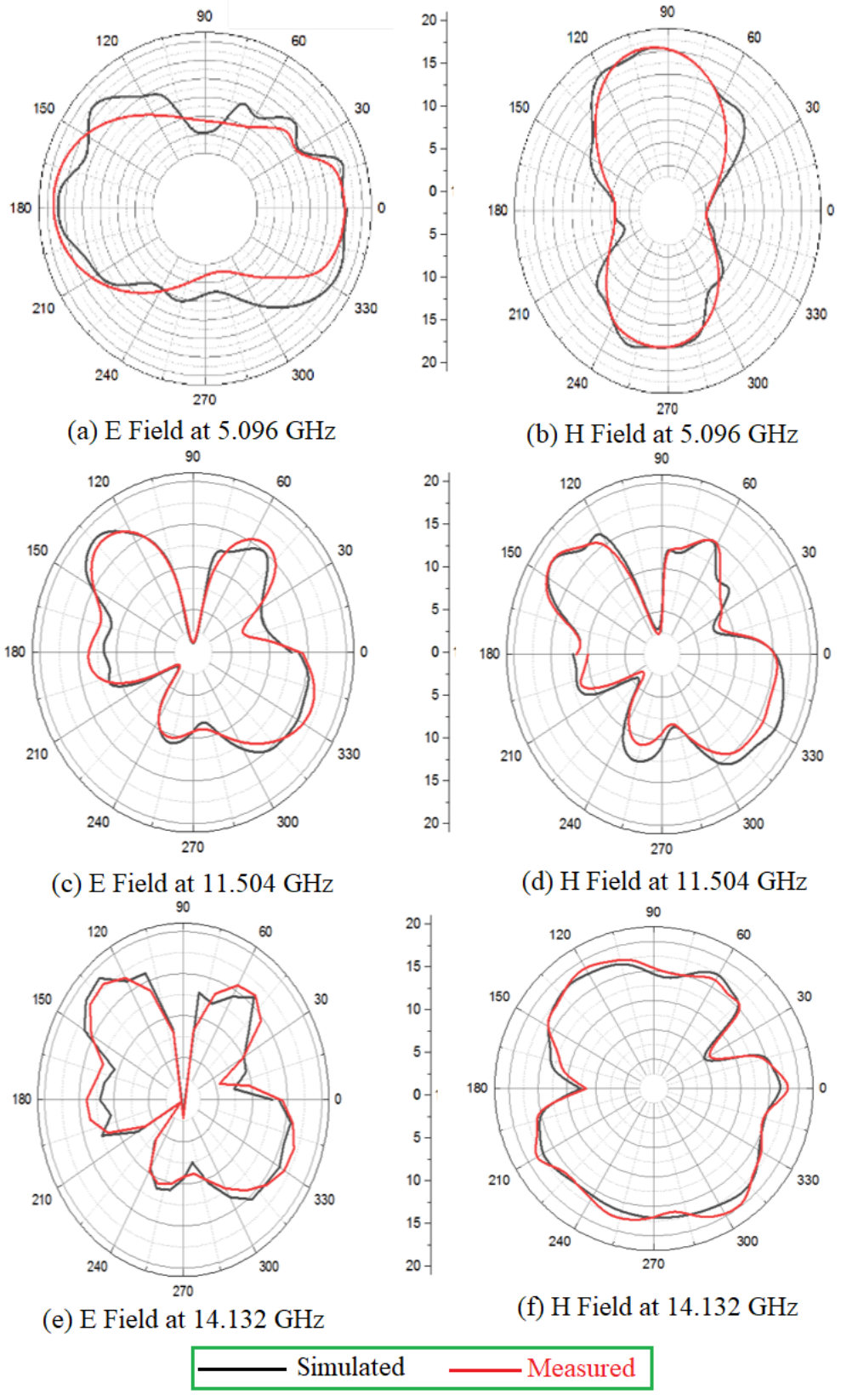
(a) E Field at 5.096 GHz
(b) H Field at 5.096 GHz
(c) E Field at 11.504 GHz
(d) H Field at 11.504 GHz
(e) E Field at 14.132 GHz
(f) H Field at 14.132 GHz
Simulated
Measured

Figure 9. Simulated and Measured Results of Polar Plot at Various Resonant Frequencies for Proposed Design

5. Conclusion and Future scope

The research mainly focuses on attaining an enhanced bandwidth in three bands of frequency using an aperture-coupled microstrip antenna. The structure has two different substrates, FR4 and RT5880, a modified defected ground structure, a patch with three rectangular apertures, and a triple Y-structured feed line. Perfect matching and coupling are attained with the help of a quarter-wave transformer in the feed line. The design was fabricated and tested, and the resultant performance was analyzed in terms of radiation parameters. The S curve shows a drastic improvement in terms of bandwidth and gain. A bandwidth of 12.6% (C band), 9.7% (X band), and 7.2% (Ku band) with a gain of 3.11 dBi, 3.75 dBi, and 4.25 dBi, respectively, is achieved. The proposed design is most suited for a 5G mobile application. Specifically, it can be used in Wi-Fi, WiMAX, speed detection, RADAR, and other 5G applications that operate within the frequency range of 14.25 GHz. An array of aperture-coupled antennas covering multiple frequency bands with improved gain and bandwidth is being considered as a future scope. Besides, the design will focus on 5G applications and miniaturization.

References

Balanis, C. A. *Antenna Theory: Analysis and Design, (3RD ED.)*. 2009.

Bancroft, R. *Microstrip and Printed Antenna Design*. 2019. doi: 10.1049/pbte083e.

Ding, Y. R and Cheng, Y. J. A tri-band shared-aperture antenna for (2.4, 5.2) ghz wi-fi application with mimo function and 60 ghz wi-gig application with beam-scanning function. *IEEE Transactions on Antennas and Propagation*, 68, 2020. ISSN 15582221. doi: 10.1109/TAP.2019.2948571.

Honari, M. M; Abdipour, A; Moradi, G; Mirzavand, R, and Mousavi, P. Design and analysis of a series-fed aperture-coupled antenna array with wideband and high-efficient characteristics. *IEEE Access*, 6, 2018. ISSN 21693536. doi: 10.1109/ACCESS.2018.2827021.

Hong, Y; Tak, J; Baek, J; Myeong, B, and Choi, J. Design of a multiband antenna for lte/gsm/umts band operation. *International Journal of Antennas and Propagation*, 2014, 2014. ISSN 16875877. doi: 10.1155/2014/548160.

Khan, Z. U; Jilani, S. F; Belenguer, A; Loh, T. H, and Alomainy, A. Empty substrate integrated waveguide-fed mmw aperture-coupled patch antenna for 5g applications. volume 2018, 2018. doi: 10.1049/cp.2018.1209.

Kim, J and Oh, J. Liquid-crystal-embedded aperture-coupled microstrip antenna for 5g applications. *IEEE Antennas and Wireless Propagation Letters*, 19, 2020. ISSN 15485757. doi: 10.1109/LAWP.2020.3014715.

Li, Y; Wang, J, and Luk, K. M. Millimeter-wave multibeam aperture-coupled magnetoelectric dipole array with planar substrate integrated beamforming network for 5g applications. *IEEE Transactions on Antennas and Propagation*, 65, 2017. ISSN 0018926X. doi: 10.1109/TAP.2017.2681429.

Liu, S; Jiang, K; Xu, G; Ding, X; Zhang, K; Fu, J, and Wu, Q. A dual-band shared aperture antenna array in ku/ka-bands for beam scanning applications. *IEEE Access*, 7, 2019. ISSN 21693536. doi: 10.1109/ACCESS.2019.2922647.

Liu, W; Chen, Z. N, and Qing, X. Metamaterial-based low-profile broadband aperture-coupled grid-slotted patch antenna. *IEEE Transactions on Antennas and Propagation*, 63, 2015. ISSN 0018926X. doi: 10.1109/TAP.2015.2429741.

Rao, Q and Johnston, R. H. Modified aperture coupled microstrip antenna. *IEEE Transactions on Antennas and Propagation*, 52, 2004. ISSN 0018926X. doi: 10.1109/TAP.2004.836415.

Wang, Z and Huang, Z. A microwave/millimeter wave dual-band shared aperture patch antenna array. *IEEE Access*, 8, 2020. ISSN 21693536. doi: 10.1109/ACCESS.2020.3040250.

Yang, Q; Gao, S; Luo, Q; Wen, L; Ban, Y. L; Yang, X. X; Ren, X, and Wu, J. Cavity-backed slot-coupled patch antenna array with dual slant polarization for millimeter-wave base station applications. *IEEE Transactions on Antennas and Propagation*, 69, 2021. ISSN 15582221. doi: 10.1109/TAP.2020.3017388.

Yun, W and Yoon, Y. J. A wide-band aperture coupled microstrip array antenna using inverted feeding structures. *IEEE Transactions on Antennas and Propagation*, 53, 2005. ISSN 0018926X. doi: 10.1109/TAP.2004.841283.

Zhang, J; Yan, S, and Vandenbosch, G. A. A miniature feeding network for aperture-coupled wearable antennas. *IEEE Transactions on Antennas and Propagation*, 65, 2017. ISSN 0018926X. doi: 10.1109/TAP.2017.2677262.

.